



FINAL YEAR PROJECT 2: DISSERTATION

Study on Shale Gas Fluid Flow in Porous Media

BY

HO CHING

14328

Dissertation submitted in partial fulfilment of the requirements for the
Bachelor of Engineering (Hons)

(Petroleum Engineering)

September 2014

Universiti Teknologi PETRONAS

Bandar Seri Iskandar

31750 Tronoh,

Perak Darul Ridzuan.

CERTIFICATION OF APPROVAL

Study on Shale Gas Fluid Flow in Porous Media

By

Ho Ching

A project dissertation submitted to the

Petroleum Engineering Programme

Universiti Teknologi PETRONAS

in partial fulfilment of the requirement for the

BACHELOR OF ENGINEERING (Hons)

(PETROLEUM ENGINEERING)

Approved by,

MOHAMMAD AMIN SHOUSHTARI

UNIVERSITI TEKNOLOGI PETRONAS

TRONOH, PERAL DARUL RIDZUAN

SEPT 2014

CERTIFICATION OF ORIGINALITY

This is to certify that I am responsible for the work submitted in this project, that the original work is my own except as specified in the references and acknowledgements, and that the original work contained herein have not been undertaken or done by unspecified sources or persons.

(HO CHING)

ABSTRACT

Extraction of shale gas which is categorized under unconventional reservoir is still remain a challenge for oil and gas industry in both technical and economical aspect. The reason being is shale possess nanopore size and this causes the difficulty for the flow of shale gas to wellbore from porous media. One of the problem faced at present is shale gas fluid flow has not been well understood and lack of this knowledge can affect the extraction and production of shale gas. Compared with conventional reservoir, the fluid flow can be described by using Darcy law. However Darcy law is not applicable to describe the fluid flow in nanopore size reservoir. Hence, this research is aimed to study and investigate the fluid flow mechanisms in shale formation. Few mathematical models from published research papers which are used to describe the shale gas fluid flow in porous media have been considered in this research. Amongst the types of non-darcy fluid flow mechanisms in shale are free gas flow, adsorption-desorption and diffusion were studied in details. Xiong et al. Model was selected and was applied to examine the apparent permeability for three different scenarios which including non-darcy flow, adsorption and surface diffusion. Sensitivity analysis of this research was presented in spreadsheet form to show the effect of the parameters on apparent permeability. There are two outcomes from the sensitivity analysis in this work. The first outcome is apparent permeability increases when pressure reduces, temperature increases and bigger pore size. The second outcome is apparent permeability with consideration non-Darcy flow only is the highest followed by apparent permeability that includes non-Darcy flow, adsorption effect and surface diffusion and finally is apparent permeability with non-Darcy flow and adsorption effect. In addition, comparison between conventional reservoir and shale gas reservoir in terms of gas generation, gas storage mechanism, produced gas types, production rate and recovery factor have also been included in this research.

ACKNOWLEDGEMENT

First and foremost, I would like to thank Universiti Teknologi PETRONAS (UTP) for coordinating this final year project and providing guidance in completing this final year project which is part of the requirement for Bachelors of Engineering (Hons) in Petroleum Engineering in UTP.

My grateful thanks also go to my supervisor, Mr. Mohammad Amin Shoushtari for his cordial support and guidance in completing this project. His willingness to guide me and spare his valuable time to give me advices was duly acknowledge and appreciated. With his guidance, I am able to complete my project smoothly and successfully.

Lastly, an honorable mention also goes to my family and friends for their guidance and sharing their valued experience to me. This final year project has truly given me the chance to learn and produce a research paper. All the guidance and assistance throughout the learning were helpful and indeed precious.

TABLE OF CONTENTS

CERTIFICATION OF APPROVAL	ii
CERTIFICATION OF ORIGINALITY	iii
ABSTRACT	iv
ACKNOWLEDGEMENT	v
TABLE OF CONTENTS	vi
LIST OF FIGURES	viii
LIST OF TABLES	ix
CHAPTER 1 INTRODUCTION	1
1.1 Background	1
1.2 Problem Statement.....	2
1.3 Objectives	3
1.4 Scope of Study.....	3
CHAPTER 2 LITERATURE REVIEW AND/OR THEORY.....	4
2.1 Shale formation geology.....	4
2.2 Comparisons between conventional reservoirs and shale reservoir	5
2.3 Porous media	6
2.4 Fluid flow mechanism in shale formation	9
2.4.1 Free gas flow	11
2.4.2 Adsorption-desorption.....	11
2.4.3 Diffusion.....	12
2.5 Xiong et al Model	13
CHAPTER 3 METHODOLOGY/PROJECT FLOW	16
3.1 Research Methodology	16
3.2 Gantt chart	17
3.3 Research Key milestone	19
3.4 Tool required	20
3.5 Modelling Methodology	20

3.6 Mathematical modelling	20
3.6.1 First Level.....	20
3.6.2 Second Level	22
3.6.3 Third Level	23
CHAPTER 4 RESULT AND DISCUSSION	25
4.1 Apparent Permeability	25
4.2 Sensitivity Analysis	26
4.2.1 Sensitivity Study of Pressure.....	27
4.2.2 Sensitivity Study of Pore Size	28
4.2.3 Sensitivity Study of Temperature.....	29
CHAPTER 5 CONCLUSION AND RECOMMENDATION.....	30
5.1 Conclusions	30
5.2 Recommendations.....	30
NOMEMCLATURES.....	31
REFERENCES.....	32
APPENDIX.....	35

LIST OF FIGURES

FIGURE 1.1 CONSUMPTION OF NATURAL GAS IN THE LAST DECADE AND PROBABLE FUTURE TREND (ENERGY INFORMATION ADMINISTRATION, 2014)	2
FIGURE 2.1 BACKSCATTER SEM IMAGE OF BARNETT SHALE KEROGEN (SONDERGELD, AMBROSE, RAI, & MONCRIEFF, 2010)	7
FIGURE 2.2 TYPE OF PORE STRUCTURE MODELS THAT EXIST IN SHALE FORMATION (FARROKHROUZ & ASEF, 2013)	7
FIGURE 2.3 PHYSICAL MODEL OF STORAGE GAS TYPE AND FLUID FLOW IN SHALE GAS POROUS MEDIA. (SWAMI, SETTARI, & JAVADPOUR, 2013)	9
FIGURE 2.4 DUAL POROSITY NETWORK MODEL IN SHALE GAS POROUS MEDIA (ALHARTHY, KOBASI, TORCUK, KAZEMI, & GRAVES, 2012)	10
FIGURE 2.5 TRIPLE POROSITY NETWORK MODEL IN SHALE GAS POROUS MEDIA. (ALHARTHY, KOBASI, TORCUK, KAZEMI, & GRAVES, 2012)	10
FIGURE 2.6 TYPE OF DIFFUSION MECHANISM. (ALLEN, APLIN, & THOMAS, 2009)	12
FIGURE 2.7 COMPARISON OF EFFECTIVE RADIUS FOR DIFFERENT PORE SIZE. (ALHARTHY, KOBASI, TORCUK, KAZEMI, & GRAVES, 2012)	14
FIGURE 4.1 GRAPH OF APPARENT PERMEABILITY FOR DIFFERENT PORE PRESSURES	27
FIGURE 4.2 GRAPH OF APPARENT PERMEABILITY FOR DIFFERENT PORE SIZES	28
FIGURE 4.3 GRAPH OF APPARENT PERMEABILITY AT DIFFERENT TEMPERATURE	29

LIST OF TABLES

TABLE 2.1 CONVENTIONAL RESERVOIR AND SHALE RESERVOIR	5
TABLE 2.2 CLASSIFICATION OF PORE SIZE (SWAMI, SETTARI, & JAVADPOUR, 2013)	8
TABLE 0.1 SENSITIVITY STUDY TABLE OF PRESSURE PARAMETER ON FIRST LEVEL OF MODELLING, K	35
TABLE 0.2 SENSITIVITY ANALYSIS OF PRESSURE PARAMETER AT SECOND LEVEL OF MODELLING, KA	36
TABLE 0.3 VISCOSITY CALCULATION FOR DIFFERENT PORE PRESSURE	37
TABLE 0.4 SENSITIVITY ANALYSIS ON PRESSURE PARAMETER ON THIRD LEVEL OF MODELLING, KAD	37
TABLE 0.5 SENSITIVITY ANALYSIS ON PORE SIZE PARAMETER ON FIRST LEVEL OF MODELLING, K	38
TABLE 0.6 SENSITIVITY ANALYSIS ON PORE SIZE PARAMETER ON SECOND LEVEL OF MODELLING, KA	39
TABLE 0.7 VISCOSITY CALCULATION FOR DIFFERENT PORE SIZES	40
TABLE 0.8 SENSITIVITY ANALYSIS ON PORE SIZE PARAMETER ON THIRD LEVEL OF MODELLING, KAD	40
TABLE 0.9 SENSITIVITY ANALYSIS ON TEMPERATURE PARAMETER ON FIRST LEVEL OF MODELLING, K	41
TABLE 0.10 SENSITIVITY ANALYSIS ON TEMPERATURE PARAMETER ON SECOND LEVEL OF MODELLING, KA	42
TABLE 0.11 VISCOSITY CALCULATION FOR DIFFERENT TEMPERATURES	43
TABLE 0.12 SENSITIVITY ANALYSIS OF TEMPERATURE PARAMETER ON THIRD LEVEL OF MODELLING, KAD	43

CHAPTER 1

INTRODUCTION

1.1 Background

The reason of this research being carried out is to model the shale gas fluid flow in porous media. Many researches on shale gas fluid flow have been investigated and published because shale gas is the future energy resources. The high demand of natural gas includes shale gas increases significantly for the usage of industrial, electricity power generation, transportation, residential and commercial. The reason being is natural gas is the cleanest burning fossil fuel and emit low percentage of carbon. Hence oil and industry started to focus on the extraction of unconventional natural gas due to high demand. Figure 1.1 illustrated natural gas consumption in the past decade and the probable future projection 25 years from now. Shale development have moved outside of United States. Country like China, Argentina, Algeria and Canada have large amount of technically recoverable shale gas. The total technically recoverable shale gas resources in China, Argentina, Algeria and Canada is 1115 trillion cubic feet, 802 trillion cubic feet, 707 trillion cubic feet, 573 trillion cubic feet respectively (EIA, 2013). However production of shale gas cannot be extracted by using conventional method such as vertical drilling method due to poor permeability. This prevents gas from flowing easily from porous media into wellbore to be produced. Therefore shale reservoir has different transport mechanism compared with conventional reservoir. Fluid flow in conventional reservoir is transported via convection method which the flow is depends on the pressure gradient and it can be described by using Darcy flow. Therefore this research is carried out in order to obtain better understanding of shale gas fluid flow in porous media.

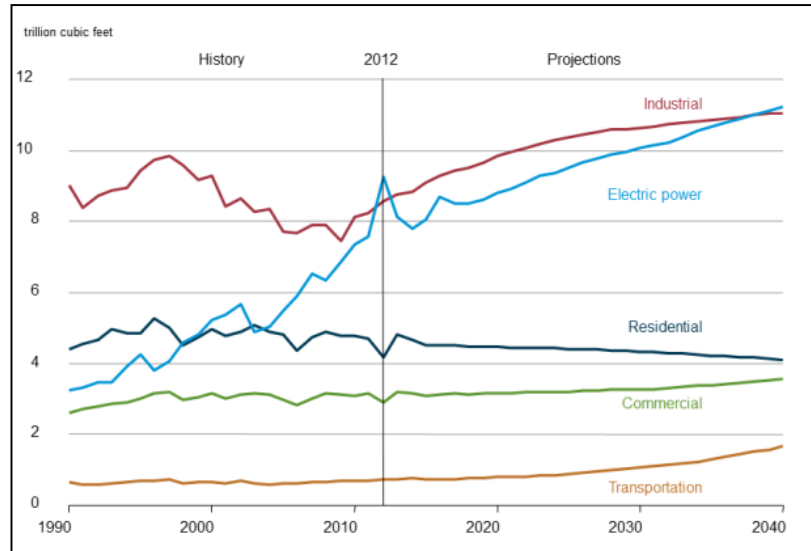


Figure 1.1 Consumption of natural gas in the last decade and probable future trend (Energy Information Administration, 2014)

1.2 Problem Statement

At present, extraction of shale gas from gas shale still remains technically and economically challenging to oil and gas sector due to shale gas is classified under unconventional reservoir which needs advance technology to extract it. The pore spaces of the shale are so small that causes difficulty for shale gas to flow from shale to wellbore for production. It was reported that the nano-pores diameter were around 1~1000nm (Wang & Reed, 2009). Although application of horizontal drilling and hydraulic fracturing technique have made shale gas production possible in past decade, however the mechanism of fluid flow in gas shale have not been well understood. This is because Darcy law cannot simply be used to describe the fluid flow in nanopores of shale gas formation (Javadpour, 2009). Besides, the effect of pore size, pore pressure and temperature on shale gas fluid flow mechanism need to be known. Hence, by developing a computer code in spreadsheet, fluid flow of shale gas in porous media can be understood better.

1.3 Objectives

The objectives of this study are:

- (a) To analyse the different types of shale gas fluid flow mechanisms in shale gas formation (porous media).
- (b) To investigate the effect of reservoir and fluid flow phenomena on apparent permeability in shale gas formation.

1.4 Scope of Study

The overall study is to analyse the different types of fluid flow mechanisms in shale gas formation. The research plan will include the study of comparison between the fluid flow in conventional and unconventional reservoir, storage and fluid flow mechanisms of shale gas such as free gas flow, adsorption-desorption and diffusion. Besides, this study is also to determine a potential mathematical modelling for shale gas fluid flow in porous media. Mathematical modelling published by researcher will be analysed prior to selection of the most plausible model to describe the shale gas fluid flow. Computer code in spreadsheet which models shale gas fluid flow in porous media will be formulated and a sensitivity analysis will then be conducted for different parameters to study the effect of reservoir and fluid flow phenomena on apparent permeability in shale gas formation. The parameters that studied in this research paper are pore pressure, pore size and temperature.

CHAPTER 2

LITERATURE REVIEW AND/OR THEORY

In the interest of study on shale gas fluid flow mechanism in porous media perfectly, the physical phenomena of the shale must be well understood. This includes the storage mechanism and fluid flow mechanism. Firstly, shale gas geology is described to give a better understanding on shale formation from geological point of view before explaining its physical phenomena.

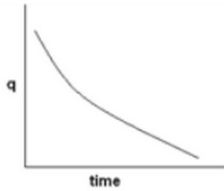
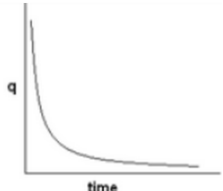
2.1 Shale formation geology

Shale is a fine-grained sedimentary rock that forms from the compaction and hardened clay, silt or mud (Farrokhrouz & Asef, 2013) ; (American Heritage Science Dictionary, 2011). It is categorized as mudrock under sedimentary category due to its composition. However, shale can be distinguished from mudrock by its physical characteristic which are shale is laminated and fissile (Gurule, 2013). Shale is the most abundantly sedimentary rock which mainly contains clay minerals, silt sized quartz and feldspar grains usually with carbonate cements. Other constituents might include pyrite and apatite, volcanic glass, iron and aluminium oxides (Farrokhrouz & Asef, 2013, p. 3). Farrokhrouz and Asef (2013) also stated that shale properties such as silt content, presence of lamination, colour, mineralogy and chemical content are highly determined by the shale depositional environment especially during compaction and diagenesis stage. During diagenesis process, the deposited sediments form to rock and organic matter transformed to kerogen. Kerogen is defined as the insoluble organic matter which has the ability to generate natural gas. High temperature and pressure exerted on the shale rock triggers chemical reaction and breakdown the organic matter into natural gas. Nevertheless due to the compaction layers of silt, clay and mud which are made up of extremely fine particle, this results in the permeability of shale is very low compared with other sedimentary rock (Gurule, 2013). Therefore, the extraction of shale gas is deemed to be uneconomical until the implementation of horizontal drilling and hydraulic fracturing in Barnett shale play.

2.2 Comparisons between conventional reservoirs and shale reservoir

According to IHS Inc. (2014), the difference between conventional reservoir and shale reservoir are as below:

Table 2.1 Conventional reservoir and shale reservoir

Characteristic	Conventional	Shale
Generation of Gas	Gas is generated in source rock before flowing to reservoir rock	Gas is generated in source rock and trapped in source rock due to low permeability
Gas Storage Mechanism	Compression	Adsorption and compression
Gas Produced	Free gas only	Adsorbed and free gas
Production Rate	Dependent on the permeability and declining reservoir pressure	Dependent on the size of fracture network near the wellbore
Recovery factor	50%-90%	5%-20%
Gas flow rate		

Source: IHS Inc. (2014)

In conventional reservoir, organic matter is stored in source rock and form hydrocarbon throughout geological period of time. The hydrocarbon is then migrates until it reaches stratigraphic or structural trap which prevent hydrocarbon from moving any further. The rock where the hydrocarbon is being stored under the trap is known as reservoir rocks. However, it is different for the case of shale gas reservoir. The hydrocarbon generated in source rock (shale rock) will not migrate to other places due to its low permeability. Therefore the source rock is same as reservoir rock for shale reservoir (Swami & Settari, 2012).

2.3 Porous media

Porous media of rock is the place where petroleum fluids are being stored. In conventional reservoir, a simple direct method which is by using equation of state can be used to determine the thermophysical properties of the petroleum fluid as a function of temperature and pressure (McCain, 1990). As for shale reservoir, the petroleum fluids have significant interaction with porous media wall (Leahy-Dios et al., 2011). The reason being is the wettability is oil wet due to kerogen in shale porous media highly possesses a chemical affinity to hydrocarbon fluid and this has given the opportunity for adsorption to occur (Ambrose et al., 2011). Speight (2013) stated that usually the bigger the surface area of organic matter, the greater the amount of absorbed methane. Javadpour, Fisher, and Unsworth (2007) explained that surface area is relative to 4 divided by diameter of the pore.

In shale gas system there are 4 types of porous media such as organic matter, nonorganic matrix, natural fracture and hydraulic fracture. For organic matter type of porous media, adsorption of gas and storage of free gases can happen in organic matter due to it has small pore size which is ranging from 5 to 1000nm. Wang, Reed, John and Katherine (2009) claimed that the porosity of organic matter can be quintupled than nonorganic matrix does. The porosity can be further increases when pore network connected to natural and hydraulic fractures. They also suggested that the fluid flow in organic matter is predominantly single phase due to organic matter is oil wet and associated pores work as nanofilters for hydrocarbon flow. By taking account of high porosity, gas slippage effect and predominantly single phase, permeability of gas in organic matter is higher compared with nonorganic matrix (Wang et al., 2009).

As can be seen in figure 2.1, kerogen which is the organic matter contains large amount of nanopores and the pores dimension in this SEM image is less than 25nm. Sondergeld, Ambrose, Rai, and Moncrieff (2010) claimed that measured porosity in kerogen is 50%. Kerogen is a gas soluble organic matter hence gas can be stored in the kerogen bulk as dissolved gas. The fraction of kerogen to total shale bulk can reach up to 40% therefore large amount of dissolved gas can be found in organic rich shale (Passey, Bohacs, Klimentidis and Sinha, 2010). Kerogen can be subdivided into nanopores and kerogen bulk.

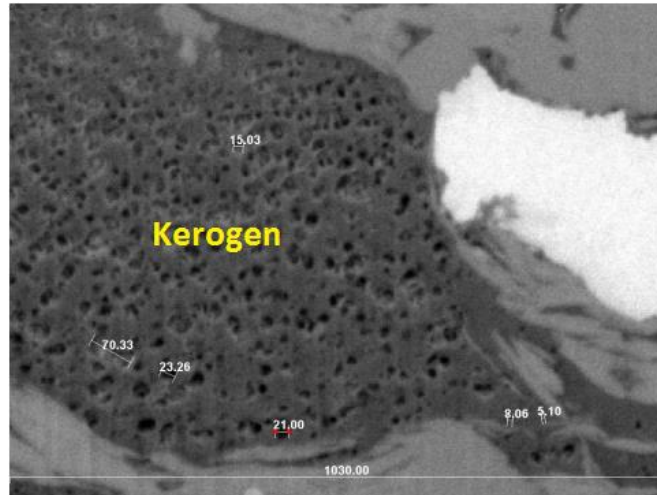


Figure 2.1 Backscatter SEM image of Barnett shale kerogen (Sondergeld, Ambrose, Rai, & Moncrieff, 2010)

The most ordinary types of storage connected pores are illustrated in figure 2.2. There are three common types of storage connected pores namely joint pores, inter-granular and vugular pores. Joint pores is formed from tension and cooling of igneous rock and hence it looks like fine fractures. Intergranular pores is the void spaces between grains in compacted material. Vugular type of pores are formed from the washed away or dissolved material which create void spaces hence it is big and irregular pores. For each types of porosity there are larger voids which is named as storage pores, and finer connecting pores which connect the storage pores (Hersir & Arnason, 2013).

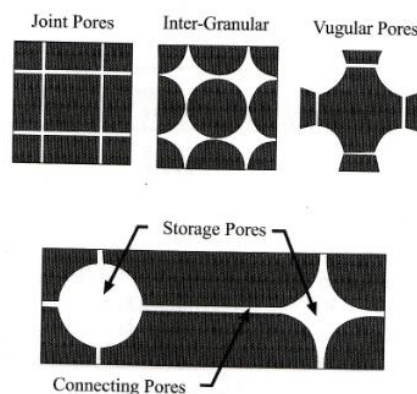


Figure 2.2 Type of pore structure models that exist in shale formation (Farrokhrouz & Asef, 2013)

It is worth noting that according to International Union of Pure and Applied Chemistry (IUPAC), classification of pore size is as shown in table 2.2. Nanopore size of shale can refer to the micropore and mesopore range of IUPAC.

Table 2.2 Classification of pore size (Swami, Settari, & Javadpour, 2013)

Pore size	Micropore	Mesopore	Macropore
Diameter	< 2nm	2nm-50nm	>50nm

It is reported that the permeability of the shale is very low which have the range about 10-100nd (Cipolla, Lolon, Erdle, & Rubin, 2010). Permeability generation is related to the characteristics of connected pores as mentioned earlier. Permeability of nanopore in shale formation can be affected by rock type, diagenesis history and burial depth (Farrokhrouz & Asef, 2013). Katsube and Williamson (1994) studied two samples of shale samples namely compacted shale and cemented shale. Diagenesis process has greater effect than mechanical compaction on pore structure at depth of greater 2.5-3.2km. This experiment concluded that the permeability reduction of cemented shale is smaller than compacted shale with depth.

2.4 Fluid flow mechanism in shale formation

Fluid flow from in gas shale is different from conventional gas reservoir. The types of fluid flow mechanisms in gas shale include free gas flow, adsorption-desorption and diffusion. Swami, Settari, and Javadpour (2013) model shale gas reservoir into a physical model as shown in figure 2.3. It is believed that shale gas can be stored as free gas in natural fractures, free gas in matrix pores, adsorbed gas on kerogen wall and dissolved gas in kerogen bulk. Gas molecules is represented by the red circles in the porous media as shown in the figure 2.3.

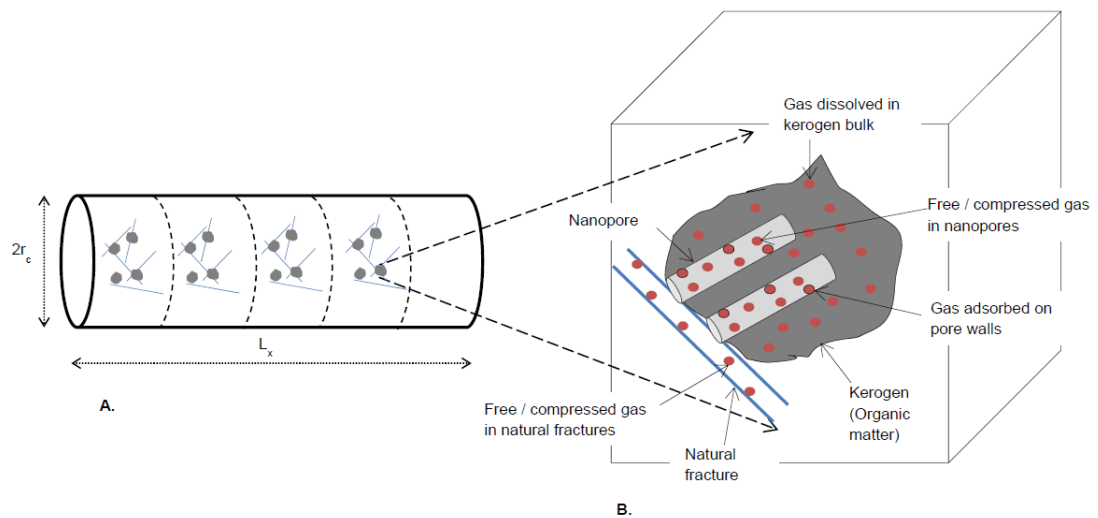


Figure 2.3 Physical model of storage gas type and fluid flow in shale gas porous media. (Swami, Settari, & Javadpour, 2013)

Javadpour (2009) reported that at equilibrium state the gas molecules filled in nanopores is known as compressed gas, the gas molecules found on the kerogen wall is known as adsorbed gas and the gas molecules distributed in the kerogen is known as dissolved gas. However when the equilibrium is affected by drilling process, the gas molecules start to flow from higher pressure zone to lower pressure zone. The compressed gases occupy in the nanopore will start to flow first and it is known as free gas flow. Consequently, the low concentration of gas molecules in nanopores causes the adsorbed gas molecules to desorb from kerogen wall and flow to nanopore to be produced. This process is known as gas desorption which will affect the concentration equilibrium between the kerogen wall and kerogen bulk and this leads to diffusion of gas molecules in the bulk of kerogen to the nanopores. Pressure can be maintained via gas diffusion process and therefore increase the production (Settari & Swami, 2012). Due to compressed gas is being stored in pores and fractures, it is easier to flow out. Therefore, the high free gas content and high free gas flow rate result in initial high

production rate and followed by long term low production rate resulted from adsorption and diffusion process (Speight, 2013). Nevertheless, these processes are overlapping to each other (Javadpour, 2009).

Alharthy, Kobaisi, Torcuk, Kazemi, and Graves (2012) demonstrated shale gas network into dual-porosity and triple-porosity network model as shown in figure 2.4 and figure 2.5 respectively.

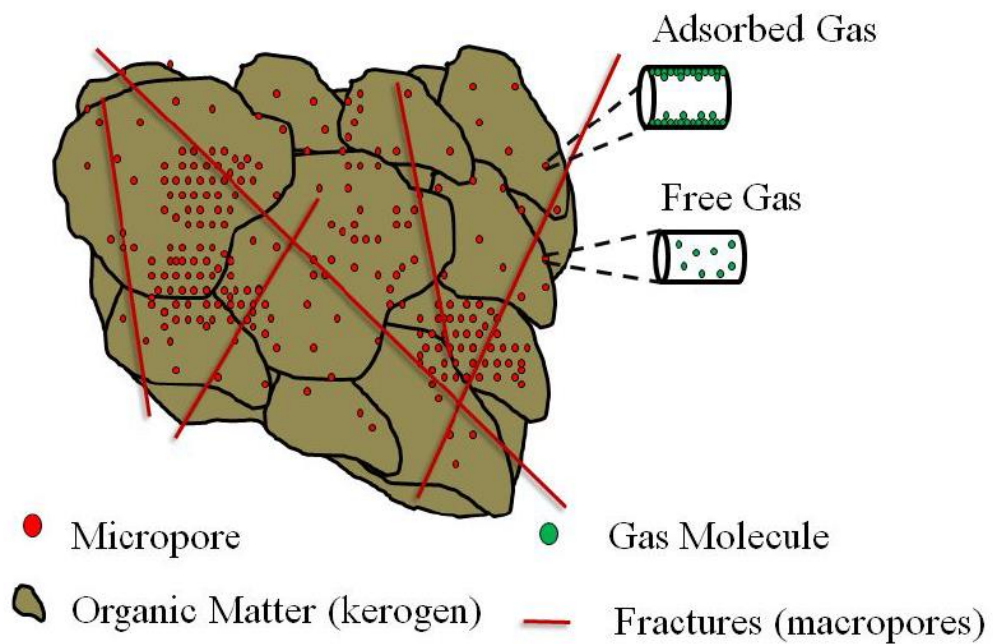


Figure 2.4 Dual porosity network model in shale gas porous media (Alharthy, Kobaisi, Torcuk, Kazemi, & Graves, 2012)

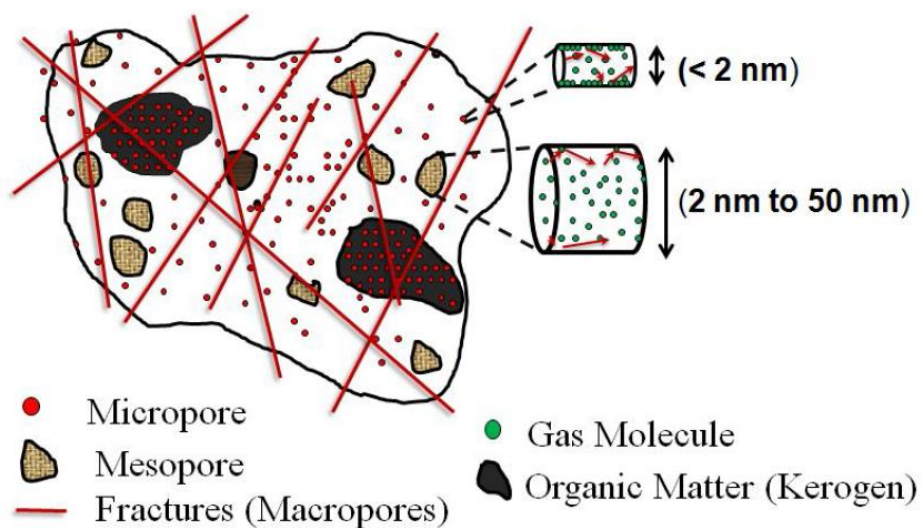


Figure 2.5 Triple porosity network model in shale gas porous media. (Alharthy, Kobaisi, Torcuk, Kazemi, & Graves, 2012)

Alharthy et al. (2012) reported that in micro level, adsorption effect is dominant while in mesolevel and macrolevel, free gas occupied in pores dominates and adsorbed gas is limited.

2.4.1 Free gas flow

Kerogen is the organic matter which has the ability to generate natural gas. The generation of gas causes the pressure build up. When the kerogen has saturated with gas molecules, gas started to liberate from the kerogen bulk to nanopore as free or compressed gas. Therefore, free gas molecules are usually found within pore spaces and fractures of the rock. When the pressure in the system reduces, free gas flow occurs first before other fluid flow mechanism (Swami & Settari, 2012). Free gas flow is characterized by non-darcy type due to the slippage effect (Wang et al., 2009).

2.4.2 Adsorption-desorption

In conventional reservoir, gas is stored by compression in pores. However in shale reservoir, some of the gas is deposited on the surface of the shale matrix by a process called adsorption. This process can be envisioned by imagining magnet with iron particles attached on it. Adsorption is different from absorption where one substance is entrapped inside the other substance (Das, 2012). According to Langmuir (1916), the gas phase is in equilibrium state when only a single layer of gas molecules adsorbed. Gas molecules collide with one another and with kerogen wall before adsorption occurs. During the collision, some gas molecules losses energy and flow with lower velocities. Irregular shape of kerogen and low gas flow velocities is then contribute for the occurrence of adsorption (Steinfeld et al., 1998). When the pressure is reduced or temperature is increasing, the attached natural gas is liberated from the surface of matrix and this process is known as desorption (Das, 2012). When the pressure is higher than the desorption pressure, the adsorbed molecules will not liberate and remains on the wall of kerogen. Consequently, the thickness of the adsorbed layer increases and impede the flow of shale gas due to decrease in pore size. In other words, both the porosity and apparent permeability decreases with the adsorbed layer thickness (Li, Li, Shi, Wang, & Wu, 2014). Adsorption-desorption of shale gas is normally described by the Langmuir (1916) Isotherm adsorption law as:

$$\frac{V}{V_m} = \frac{bP}{1+bP} \dots\dots\dots (2.1)$$

Where V_m is representing the maximum amount of gas adsorbed on wall of kerogen, $b=1/p_L$ is Langmuir pressure reciprocal and p_L is expressed as the pressure at which volume of adsorbed gas reach maximum. Thickness absorbed molecular layer and nano-pore radius of effective flow can be obtained by using Langmuir equation.

2.4.3 Diffusion

Gas diffusion plays an important role for low permeability reservoir. Diffusion influence is stronger when there is low permeability (Wei, Duan, Fang, Wang, Yu & Yu, 2012). Diffusion occurs after desorption of natural gas escapes from matrix surface. According to Allen, Aplin, and Thomas (2009), the rate of diffusion is dependent on the ratio of gas size to pore size and this ratio determines the type of diffusion mechanism in porous media. Diffusion mechanism includes gas diffusion, Knudsen diffusion, surface diffusion and activated diffusion. These mechanisms are illustrated in figure 2.6.

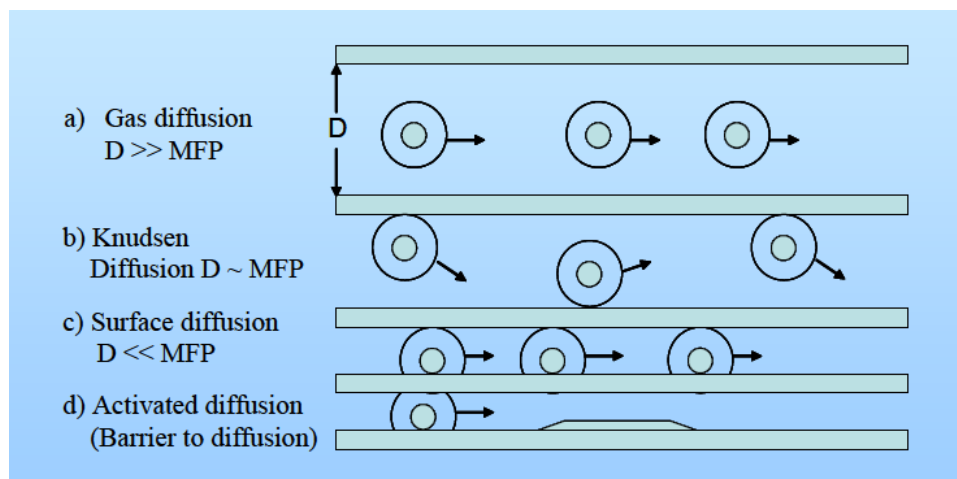


Figure 2.6 Type of diffusion mechanism. (Allen, Aplin, & Thomas, 2009)

Gas diffusion occurs when the diameter of the pore is greater than the mean flow path of the gas molecules and therefore the number of collision between the gas molecules is higher than collision with pore wall. Knudsen diffusion happens when the gas molecules mean free path is decreasing and the chances of collision to pore surfaces happen is more than the collision between the gas molecules (Roque-Malherbe,2007). When the pore diameter is smaller than the mean free path, gas molecules tends to adsorb at the surface of the matrix. This process is known as surface diffusion. Activated diffusion is the barrier to diffusion.

Branauer (1943) stated that gas molecules adsorbed on the surface of solid are free to move over one another on the surface during surface diffusion. The movement of the molecules is due to the surface concentration gradient. Gas molecules initially adsorbed on the low energy site. It vibrates on the surface and can hop on the surface with a specified velocity. As a result, it contributes to the surface migration within the adsorbed layer. When it acquires a sufficient energy, gas molecules will escape from the adsorbed layer and return to gaseous phase.

2.5 Xiong et al Model

In this model, author adopted a model of Beskok and Karniadakis (1999) which studies the flow in nano circular tube size in order to describe the gas transport in nanopore. Methane gas is chosen to characterize the gas flow in nano porous media due to methane gas has a significant adsorption characteristic. The diameter of the methane molecules is 0.38nm. There are two adsorption impacts on the gas flow namely reduction of pore volume which hinder the flow of the gas and transport mechanism within the adsorbed layer. Xiong et al Model assumes a Langmuir adsorption model which describes monolayer adsorption. This model also introduced the three level of modelling. The first level of modelling is only non-Darcy flow impact on apparent permeability is considered which given by

$$K = K_{\infty} f(K_n) \dots \dots \dots (2.2)$$

Intrinsic permeability, K_{∞} is used in this equation which defined as the permeability for the flow of a viscous non-reacting ideal liquid. $f(K_n)$ term is used so that permeability is applicable for all types of flow regime. No reduction in pore volume and pore radius since adsorption effect is not considered in this level of modelling.

At second level of apparent permeability modelling, adsorption effect is considered together with non-Darcy flow. Reduction of pore volume can be seen and hence effective radius is used instead of pore radius. It can be concluded that, apparent permeability in the second level of modelling is pressure dependent. Figure 2.7 shows that the effect of radius reduction of smaller pore size is more significant than in larger pore size.

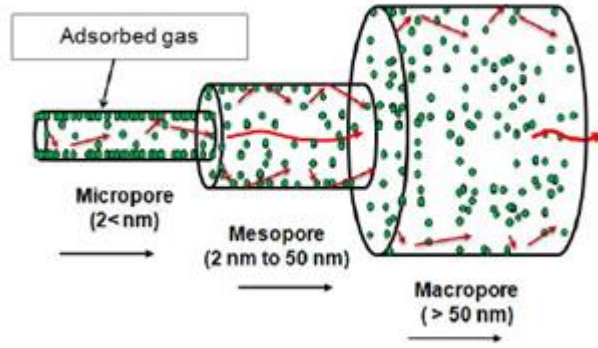


Figure 2.7 Comparison of effective radius for different pore size. (Alharthy, Kobaisi, Torcuk, Kazemi, & Graves, 2012)

The second level of modelling is given by:

$$K_a = K_{a\infty}(P)f(K_n')$$
 (2.3)

At the third level of apparent permeability modelling, surface diffusion effect is incorporated with non-Darcy flow and adsorption effect. According to Volmer and Adhikari (1925), the surface diffusion is caused by the surface concentration gradient. The mechanism of surface flux is described as hopping mechanism where a gas molecules is adsorbed on a low energy surface and it will migrate between the gas molecules. Once it acquires enough energy to escape from the surface, it turns into free gas molecules to be produced. Most of the time, the exchange rate of the absorbed gas to free gas is higher than the surface migration flow rate. Therefore, surface diffusion is another contributor for the gas flow (Rlando, 2007). The third level of modelling is given by

$$K_{ad} = K_a + D\mu \frac{MC_{a\max}P_L}{(P+P_L)^2} (1 - \phi_{eff})$$
 (2.4)

Lee, Gonzalez, and Eakin Correlation is used to calculate the viscosity parameter. Viscosity parameter is pressure and temperature dependent. However, only pressure is considered in this research. The Lee, et al. correlation (1966) which is based on the hydrocarbon gas molecular weight, gas density at specific temperature and pressure and temperature yields quite accurate result for natural gas with low nonhydrocarbon content. The pressure range for using this correlation is between 100psia to 8000psia and the temperature ranges from 100 deg F to 340 deg F. Equation for viscosity is given by

$$\mu = 10^{-4}K \exp(X\rho^Y) \dots\dots\dots (2.5)$$

The equation of parameter of K, X and y is presented in Chapter 3. Pressure is altered in the density parameter to see the effect on the pressure on viscosity. The equation for density is given by

$$\rho = \frac{1}{62.37} \frac{PM}{ZRT} \dots\dots\dots (2.6)$$

All the symbols will be explained in nomenclature in page 31.

CHAPTER 3

METHODOLOGY/PROJECT FLOW

This chapter covers the research methods and project activities. Project activities is shown by using project key milestone, project timeline is presented by using Gantt-chart and required tools are elaborated in this chapter.

3.1 Research Methodology

The overall research methodology is preliminary research, implementation stage, analysis of result and discussion stage and lastly is report writing and documentation work.

Preliminary research

Figuring out the theory of the fluid flow mechanism in shale gas porous media such as non-darcy flow, adsorption-desorption, diffusion process occur in porous media, find out the programme to be used in order to transform modelling equation into computer code and lastly is to research on the approaches to fulfil the work requirement.

Implementation stage

This stage is to carry out the determined method in order to obtain the findings. A Excel spreadsheet is chose as the tool which is adequate for transforming an algebraic model into computer language.

Analysis of result and discussion

Obtaining the results from the spreadsheet and validate it, discussing the result by using graph to have clearer picture, ensuring objectives have achieved.

Report writing and documentation

Compilation of all the findings and outcome of the project as well as the interpretation of the result, literature review and finally conclusion and recommendation.

3.2 Gantt chart

Final Year Project 1

Detail/Week	1	2	3	4	5	6	7	8	9	10	11	12	13	14
Selection of Project	■	■	■											
Preliminary Research Work				■	■	■								
Submission of Extended Proposal								★						
Proposal Defence									■					
Project work Continues									■	■	■	■		
Submission of Interim Draft													★	
Submission of Interim Report														★



Deliverable



Progress

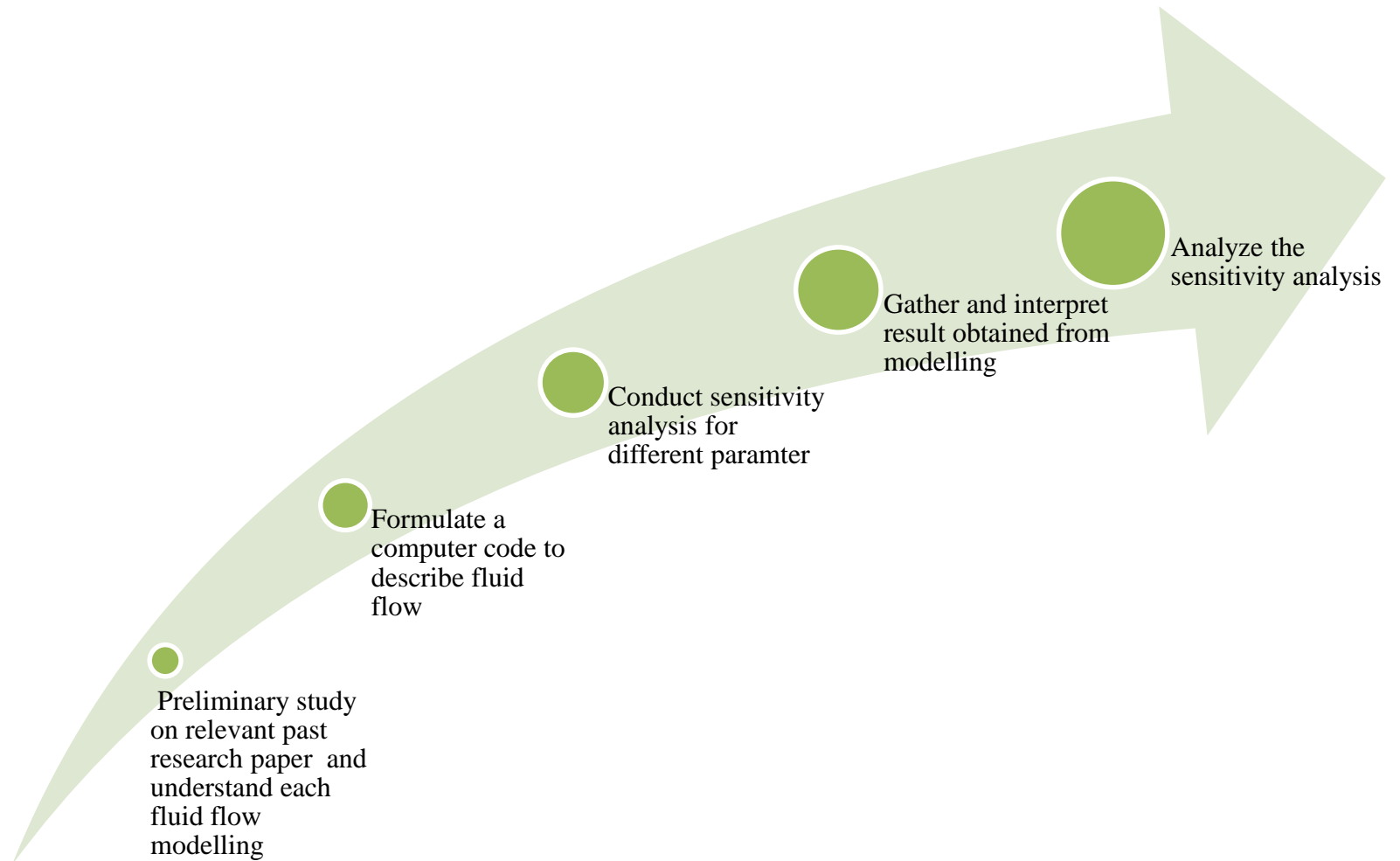
Final Year Project 2

Detail/Week	1	2	3	4	5	6	7	8	9	10	11	12	13	14	15
Project work continuous	■	■	■	■	■	■	■								
Submission of progress report							★								
Project work continuous								■	■	■	■	■	■		
Pre-SEDEX									★						
Submission of Final Daft												★			
Submission of Technical Paper												★			
Viva														★	
Submission of Project Dissertation (Hardbound)															★

★ Deliverable

■ Progress

3.3 Research Key milestone



3.4 Tool required

The required tool for this project is Microsoft Excel. It is used to transpose the identified model which is Xiong et al Model into a spreadsheet. Microsoft Excel spreadsheet operates on data which filled by the user and organized in rows and column. Results of the formulae will be executed and displayed based on the input value. Stored value can be edited and effect on the calculated value can be observed. Lastly, the behaviour and pattern of the data can be illustrated in the form of chart and graph for clearer picture.

3.5 Modelling Methodology

In this project, fluid flow of shale gas in porous media will be modelled by using Microsoft Excel. Published research papers will be reviewed to analyse the different shale gas fluid flow models. Amongst the models, the most plausible model will be identified prior to develop a spreadsheet based on the identified model. Lastly, a sensitivity analysis will be conducted on different parameters followed by gathering and analysing the result.

3.6 Mathematical modelling

The flow mechanisms of shale gas in porous media include free gas flow, adsorption and gas diffusion. In order to model the fluid flow of shale gas in porous media, a generalized model of Beskok and Karniadakis (1999) was adopted by Xiong et al. (2012) which describe the flow in a narrow circular tube for by taking account of apparent permeability, gas desorption and surface diffusion.

There are three levels of transport modelling in order to investigate the flow in single capillary tube with uniform length (Xiong et al., 2012). The level and equation is as below:

3.6.1 First Level

At the first level, non-Darcy flow effect is the only one effect considered in the apparent permeability (Xiong et al., 2012).

$$K = K_{\infty} f(K_n) \dots\dots\dots (3.1)$$

Assumption made is the complexities of the pore geometry are described by the term of intrinsic permeability, K_{∞} and $f(K_n)$ is kept in the same form by substituting the radius of the pore.

In order to obtain equation 3.1, equations as follows need to be executed.

Equation for Intrinsic permeability, K_∞ :

Hydraulic radius, R_h is the same throughout developing the spreadsheet due to no adsorption effect is considered in the apparent permeability. Equation 3.2 represent intrinsic permeability.

$$K_\infty = \frac{R_h^2}{8} \dots\dots\dots(3.2)$$

Equation for Ideal gas mean-free path, λ :

Boltzmann constant, k_B is assumed to be $1.3806504 \times 10^{-23}$ J/K and molecules diameter, d_m is assumed to be 0.38 nm in the developed spreadsheet. T is temperature in Kelvin unit and P is pressure in Pascal unit.

$$\lambda = \frac{k_B T}{\sqrt{2} \pi P d_m^2} \dots\dots\dots(3.3)$$

Equation for Knudsen Number, K_n :

Knudsen number remains constant in the developed spreadsheet which is the ratio of ideal gas mean-free path to hydraulic radius.

$$K_n = \frac{\lambda}{R_h} \dots\dots\dots(3.4)$$

Equation for Rarefaction coefficient, α :

$$\alpha = \frac{128}{15\pi^2} \tan^{-1}(4K_n^{0.4}) \dots\dots\dots(3.5)$$

Equation for $f(K_n)$:

B is assumed to be -1 for full slippage. Knudsen number, K_n is taken from equation 3.4 and rarefaction coefficient, α is taken from equation 3.5.

$$f(K_n) = (1 + \alpha K_n) \left(1 + \frac{4K_n}{1 - bK_n}\right) \dots\dots\dots(3.6)$$

3.6.2 Second Level

At the second level of modelling, adsorption is taken into account. Effective radius is dependent on the current pressure condition. Therefore, intrinsic permeability becomes pressure dependent (Xiong et al., 2012). The apparent permeability for second level is given by

$$K_a = K_{a\infty}(P)f(K_n') \dots\dots\dots(3.7)$$

In order to obtain equation 3.7, equations as follow need to be executed.

Equation for effective radii, R_{eff} :

Langmuir pressure is assumed to be 1800 Psia. Effective radii is the radius in the presence of adsorbed gas molecules and it is the result of subtraction of methane gas molecules from the hydraulic radius.

$$R_{eff} = R_h - d_m \frac{P/P_L}{1+P/P_L} \dots\dots\dots(3.8)$$

Equation for Effective porosity, Φ_{eff} :

In porous media, loss of radius is same as loss of porosity, hence effective porosity is in term of effective radii.

$$\Phi_{eff} = \frac{R_{eff}^2}{R_h^2} \dots\dots\dots(3.9)$$

Equation for Knudsen number, K_n' :

$$K_n' = \frac{\lambda}{R_{eff}} \dots\dots\dots(3.10)$$

Equation for $f(K_n')$:

$$f(K_n') = (1 + \alpha K_n')(1 + \frac{4K_n'}{1-bK_n'}) \dots\dots\dots(3.11)$$

3.6.3 Third Level

For the third level of modelling, diffusion in the adsorbed layer is incorporated with non-darcy flow and desorption effect as presented in equation 3.12 (Xiong et al., 2012).

$$K_{ad} = K_a + D\mu \frac{MC_{a\max}P_L}{(P+P_L)^2} (1 - \phi_{eff}) \dots\dots\dots(3.12)$$

In order to obtain equation 3.12, equation as follow need to be executed.

Equation for methane molecular weight, M:

The specific gravity of methane has the value of 0.5537.

$$M = 28.967 \gamma_g \dots\dots\dots(3.13)$$

Equation for viscosity, μ :

Viscosity is calculated by using Lee, Gonzalez, and Eakin Correlation. The Lee, et al. correlation which is based on the temperature, gas density at specific temperature and pressure, and hydrocarbon gas molecular weight. Equation for viscosity is given by:

$$\mu = 10^{-4}K \exp(X\rho^Y) \dots\dots\dots(3.14)$$

The equations for all the parameter in equation 3.14 are shown as follow

$$K = \frac{(9.379+0.01607M)T^{1.5}}{209.2+19.26M+T} \dots\dots\dots(3.15)$$

$$X = 3.448 + \frac{986.4}{T} + 0.01009M \dots\dots\dots(3.16)$$

$$Y = 2.447 - 0.2224X \dots\dots\dots(3.17)$$

Equation for density, ρ :

$$\rho = \frac{1}{62.37} \frac{PM}{ZRT} \dots\dots\dots(3.18)$$

Equation for compressibility factor, Z:

An analytical method is used to calculate the compressibility factor by using the CNGA equation as shown follow:

$$Z = \frac{1}{1 + \left(\frac{P \times 344400 \times 10^{1.785G}}{T^{3.825}} \right)} \dots\dots\dots(3.19)$$

Sensitivity analysis with different parameters namely pore pressure, pore size and temperature was carried out. Each parameter value with the corresponding apparent permeability is presented to show their effects on apparent permeability. The results were illustrated in the form of graph for comparison purpose and to show the behaviour of the particular fluid mechanisms of shale gas in porous media.

CHAPTER 4

RESULT AND DISCUSSION

This chapter covers the result of the spreadsheet on the fluid flow in shale gas in porous media and discuss the findings from the results. Results are tabulated in table form by using Microsoft Word Excel spreadsheet and different levels of modelling are presented in different sheet of spreadsheet. Each parameter for sensitivity analysis is differentiated by different tab colour. All the input data, first level of modelling which only consider non-darcy flow, second level of modelling which consider both non-darcy flow and adsorption and lastly third level of modelling which combine all the transport mechanism such as non-darcy flow, adsorption and surface diffusion is presented systematically in excel together with the plotted graph.

4.1 Apparent Permeability

In the comparison of the three levels of modelling, first level of modelling which only consider non-Darcy flow yields highest apparent permeability as no reduction in pore volume. When adsorption pressure is considered together with non-Darcy flow, adsorbed gas is harder to be produced compared to the gas in pore where no adsorption take place. It takes time for the adsorbed gas molecules to be produced thoroughly. In addition, the reduction of pore volume due to the adsorption process causes the apparent permeability decreases. Therefore, permeability of first level of modelling is higher than the second level of modelling. As for the third level of modelling which consider surface diffusion, the permeability is slightly higher than the second level modelling due to desorbed gas molecules will convert to gaseous phase once it possessed adequate amount of energy and escape from the surface. Hence the sequence of apparent permeability from highest to lowest is apparent permeability with only non-Darcy flow, non-Darcy flow with adsorption and surface diffusion in addition to non-Darcy flow with adsorption.

4.2 Sensitivity Analysis

In order to understand the behaviour of the fluid flow in nanopore in term of apparent permeability, value of different parameter is edited to analyse its effect on apparent permeability. This analysis is known as sensitivity analysis. Sensitivity analysis is done by using spreadsheet and results obtained are presented in a line graph for better understanding. There are three parameters have been selected and examined its effect on apparent permeability namely pore size, pore pressure and temperature. For this sensitivity analysis, ten value of pressure, pore sizes and temperatures are selected in order to examine the effect of various range of certain parameter on apparent permeability. Constant value of other parameter is imported from the first page of the spreadsheet into the equation and some of the value of parameter is executed in the same page of spreadsheet depending on the level of modelling. Apparent permeability is shown in the last column for every level of modelling.

4.2.1 Sensitivity Study of Pressure

Pressure plays an important role in determining the permeability of shale gas in porous media. Different pressure is input into the spreadsheet to study the effect of pressure on the permeability of shale gas. Pore pressure is used instead of effective pressure due to adsorption is determined by pore pressure and effective pressure is not suitable in describing permeability which varies with pressure in the case of adsorption. Ten different pore pressures which ranges from 500psia to 5000psia with increment of 500psia, pore size of 2nm, temperature of 350K are input into the spreadsheet and the corresponding apparent permeability are obtained. Figure 4.1 shows the effect of pressure on apparent permeability for three level of modelling. The graph shown that the higher the pore pressure, the lower the apparent permeability for all the three levels of modelling. For the first level of modelling (K) which without considering adsorption effect, the reason apparent permeability increases with decrease in pressure is gas molecules starts to flow to the lower pressure zone. For the second level of modelling (Ka), as the pressure increases, more adsorbed molecules is attached on the wall of the organic matter which reduces porosity and permeability. When the pressure depleted, adsorbed gas starts to desorb from the organic surface lead to increase in apparent permeability. For the third level of modelling case (Kad), surface diffusion improves the apparent permeability when pressure reduces. The results of first level, second level and third level of modelling from spreadsheet are tabulated in Appendix Table 3, Table 4 and Table 6 respectively. Viscosity calculation for third level of modelling is tabulated in Appendix Table 5.

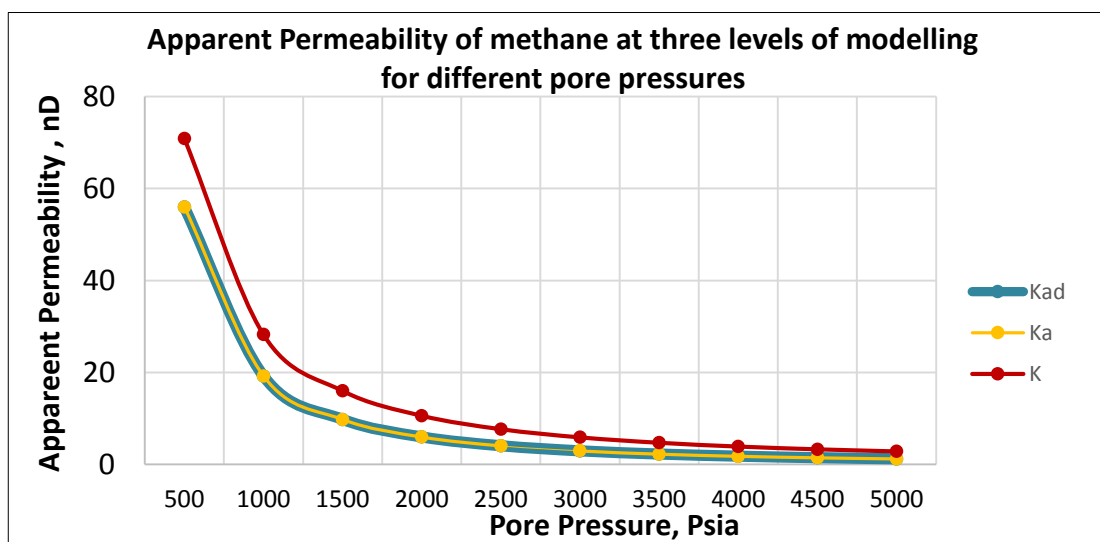


Figure 4.1 Graph of apparent permeability for different pore pressures

4.2.2 Sensitivity Study of Pore Size

By altering the value of pore size in spreadsheet, the behaviour of permeability can be known for different value of pore size in shale formation. Ten pore sizes are selected to examine the effect of the pore size on apparent permeability. Hydraulic pore radius ranges from 1nm to 10nm with increment of 1nm, pore pressure of 500psia, temperature of 350K are used for sensitivity study of pore size. Figure 4.2 shows the effect of pore sizes on apparent permeability for three level of modelling. The result obtained is the larger pore size yields higher apparent permeability. It can be seen that for all the three levels of modelling, the apparent permeability of bigger pore size is higher than the apparent permeability of smaller pore size. For second level modelling (K_a), the total pore spaces taken by adsorbed molecules to the total pore spaces for bigger pore size is smaller due to larger pore size in diameter. Hence, the volume taken by adsorbed layer becomes less important and therefore it has a better permeability than small pore size. For third level of modelling (K_{ad}), the contribution from surface diffusion is negligible in larger size therefore the apparent permeability of large pore size is much higher. As pore size reducing, surface diffusion enhances the permeability significantly at low pressure. It is concluded that larger pore size possess higher permeability. The results of first level, second level and third level of modelling from spreadsheet are tabulated in Appendix Table 7, Table 8 and Table 10 respectively. Viscosity calculation for third level of modelling is tabulated in Appendix Table 9.

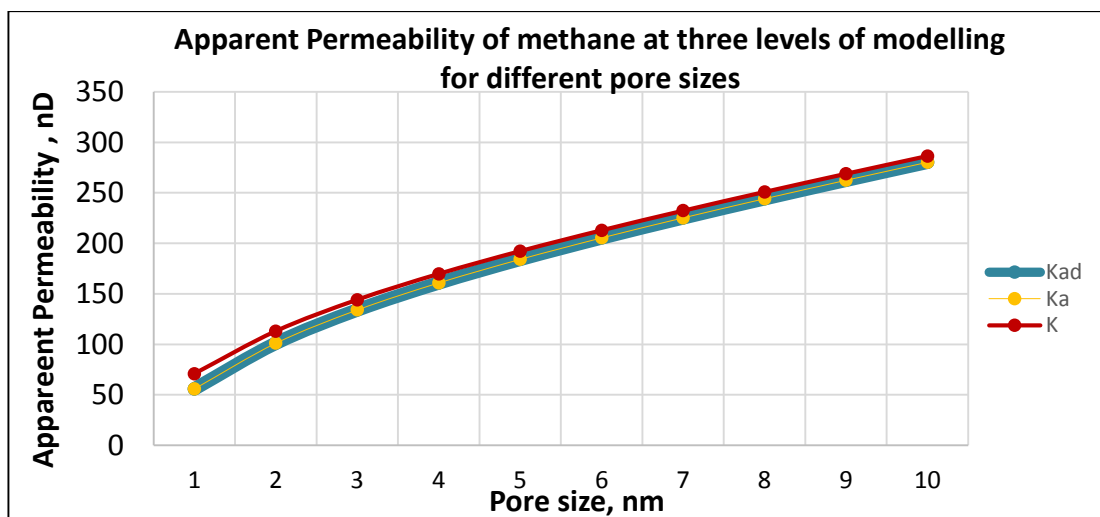


Figure 4.2 Graph of apparent permeability for different pore sizes

4.2.3 Sensitivity Study of Temperature

In this sensitivity study, ten different temperatures are used to study the effect of temperature on apparent permeability. Temperature ranges from 310K to 355K with increment of 5K, pore size of 2nm and pore pressure of 500 psia are selected for the temperature sensitivity study. Figure 4.3 shows the effect of temperature on apparent permeability for three level of modelling. The result obtained shown that the higher the temperature, the higher the apparent permeability. As mentioned surface diffusivity is affected by temperature, the result shown that the higher the temperature, the higher the surface diffusivity and therefore apparent permeability is higher when the temperature increases. Temperature has the less effect of mean free path, therefore it can be seen that the apparent permeability varies not much. This is due to shale gas is an isothermal in nature therefore desorption process does not highly affected by temperature. The results of first level, second level and third level of modelling from spreadsheet are tabulated in Appendix Table 11, Table 12 and Table 14 respectively. Viscosity calculation for third level of modelling is tabulated in Appendix Table 13.

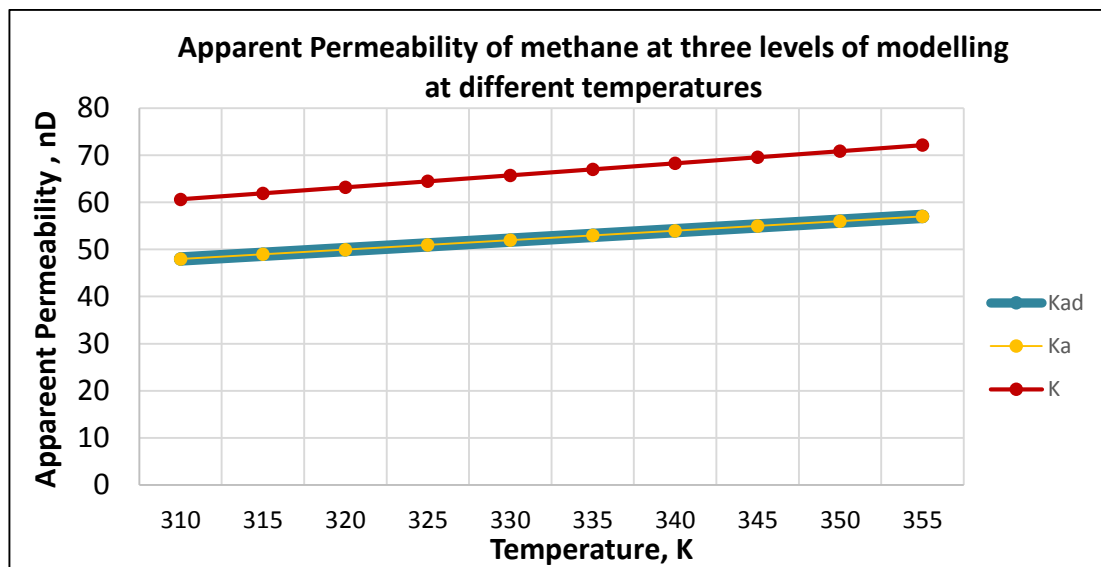


Figure 4.3 Graph of apparent permeability at different temperature

CHAPTER 5

CONCLUSION AND RECOMMENDATION

5.1 Conclusions

A total of 23 research papers were being referred and cited to strengthen this research which entitled of Study on Shale Gas Fluid Flow in Porous Media. The entire project can be summarized as follow:

- The objective of this research paper has been achieved in such that shale gas fluid flow mechanisms were identified and studied. The types of shale gas non-Darcy fluid flow mechanism are free gas flow, adsorption-desorption and diffusion.
- To fulfil the objectives of this research, effect of pore size, pore pressure and temperature on apparent permeability in shale gas formation have been investigated through sensitivity analysis.
 - ✓ Apparent permeability is higher when pore pressure decreases, bigger pore size and at higher temperature
 - ✓ Apparent permeability with consideration non-Darcy flow only is the highest followed by apparent permeability that includes non-Darcy flow, adsorption effect and surface diffusion and finally is apparent permeability with non-Darcy flow and adsorption effect.
- A better insight of shale gas fluid flow mechanism have been obtained and it hopefully will bring benefits to oil and gas industry.
- This project is feasible by taking account of the time constraint and the capability of final year student with the assistance from supervisor.

5.2 Recommendations

This research can be further improved by including other mathematical modelling on study of different type of shale gas fluid flow mechanism in porous media. In addition, this work is favourable to be extended by using actual shale gas formation field data in order to model the fluid flow mechanisms in shale gas porous media.

NOMEMCLATURES

- $C_{a\max}$ - Adsorbed phase concentration
- d_m - Molecules diameter
- D - Surface diffusivity
- K – Apparent permeability for first level of modelling
- Ka - Apparent permeability for second level of modelling
- Kad - Apparent permeability for third level of modelling
- $K_{a\infty}$ - Adsorption modified intrinsic permeability
- K_∞ - Intrinsic permeability
- k_B - Boltzmann constant
- K_n - Knudsen number with pore radius
- K_n' - Knudsen number with effective radius
- M - Molecular weight of Methane
- P_L - Langmuir pressure
- T – Temperature
- R_{eff} - Effective radii
- R_h - Pore hydraulic radius

Greek symbols

- α - Rarefaction coefficient
- μ - Real gas viscosity
- λ - Ideal gas mean-free path
- Φ_{eff} - Effective porosity

REFERENCES

- Alharthy, N., Kobaisi, M., Torcuk, M., Kazemi, H., & Graves, R. (11-14 November, 2012). *Physic and Modelling of Gas Flow in Shale Reservior*. p. 4.
- Allen, N., Aplin, A., & Thomas, M. (2009). Introduction to Shale Gas Storage. *Power Point Slide*. Retrieved from http://www.slideshare.net/kyqoy2/allen-2009-introshalegasstorage?qid=053febd3-4dde-404d-9870-5100ea271bbe&v=default&b=&from_search=2
- Ambrose, R., Hartman, R., & Akkutlu, I. (2011). Multi-component Sorbed Phase Considerations for Shale Gas-in-Place Calculations. *Paper SPE 141416 presented at the SPE Production and Operations Symposium held in Oklahoma City, Oklahoma, 27-19 March*.
- American Heritage Science Dictionary. (2011). (A. H. Dictionaries, Ed.)
- Beskok, A., & Karniadakis, G. (1999). *A Model for Flows in Channels, Pipe and Ducts at Micro and Nano Scales*.
- Brunauer, S. (1943). The Adsorption of Gasses and Vapors. *Oxford University Press Vol 1*.
- Cipolla, C., Lolon, E., Erdle, J., & Rubin, B. (2010). Reservoir Modelling in Shale Gas Reservoirs. *SPE*, 638.
- Das, J. (2012). Extracting Natural Gas Through Desorption in Shale Reservoirs. *Tech 101*, 8(1), 11.
- Energy Information Administration. (13 June, 2013). Retrieved from <http://www.eia.gov/analysis/studies/worldshalegas/>
- Energy Information Administration. (3 July, 2014). Projected Increased in Production of Shale Gas. Retrieved from <http://www.bseec.org/articles/projected-increase-production-shale-gas>
- Farrokhrouz, M., & Asef, M. (2013). *Shale Engineering Mechanics and Mechanisms*. London, UK: CRC Press/Balkema.

- Freeman, C. (2013). Study of Multi-scale Transport Phenomena in Tight Gas and Shale Gas Reservoir Systems.
- Gurule, K. (11 June, 2013). *Shale Gas*. Retrieved from <http://frackwire.com/shale-gas/>
- Hersir, G. P., & Arnason, K. (2013). Resistivity of Rocks. 3.
- IHS Inc. (2014). *Shale Gas Properties*. Retrieved from http://www.fekete.com/SAN/WebHelp/FeketeHarmony/Harmony_WebHelp/Content/HTML_Files/Reference_Material/General_Concepts/Shale_Properties.htm
- Javadpour, F. (August, 2009). Nanopores and Apparent Permeability of Gas Flow in Mudrocks(Shales and Siltstone). *Journal of Canadian Petroleum Technology*, 48.
- Javadpour, F., Fisher, D., & Unsworth, M. (2007). Nanoscale Gas Flow in shale Gas Sediments. *Journal of Canadian Petroleum Technology*, 46(10), 55-61.
- Katsube, T., & William, M. (1994). Effects of Diagenesis on Shale Nano-pore Structure and Implication for Sealing Capacity. *Clay Mineral*.
- Langmuir, I. (1916). *The Constitution of Fundamental Properties of Solids and Liquids*.
- Leahy-Dios, A., Das, M., Agarwal, A., & Kaminsky, R. (2011). Modeling of Transport Phenomena and Multicomponent Sorption for Shale Gas and Coalbed Methane in an Unstructured Grid Simulator. *Paper SPE 149352*.
- Li, Y., Li, W., Shi, J., Wang, H., Wu, L., & Teng, S. (2014). A Nano-Pore Scale Gas Flow Model for Shale Gas Reservoir. *SPE*.
- Li, Y., Li, X., Shi, J., Wang, H., & Wu, L. (2014). A Nano-Pore Scale Gas Flow Model for Shale Gas Reservoir. *SPE*.
- McCain, W. (1990). The Properties of Petroleum Fluids. *Tulsa: Penn Well Publishing Company*, 83.
- Passey, Q., Bohacs, K., Esch, E., Klimentidis, R., & Sinha, S. (2010). From Oil-Prone Source Rock to Gas-Producing Shale Reservoir-Geologic and Petrophysical Characterization of Unconventional Shale-Gas Reservoirs. *SPE*.

- Roque-Malherbe, R. M. (2007). *Adsorption and Diffusion in Nanoporous Materials*. CRC Press.
- Settari, A., & Swami, V. (2012). A Pole Scale Gas Flow Model for Shale Gas Reservoir . *SPE*.
- Sondergeld, C., Ambrose, R., Rai, C., & Moncrieff, J. (2010). Micro-Structural Studies of Gas Shales. *SPE*.
- Speight, J. G. (2013). *Shale Gas Production Processes*. USA: Gulf Professional Publishing.
- Steinfeld, J., Francisco, T., & Hase, W. (1998). *Chemical Kinetics and Dynamics*.
- Swami, V., Settari, A., & Javadpour, F. (2013). A Numerical Model for Multi-Mechanism Flow in Shale Gas Reservoirs with Application to Laboratory Scale Testing. *SPE*.
- Volmer, M., & Adhikari, G. (1925). *Physik*.
- Wang, F., Reed, R., John, A., & Katherine, G. (2009). Pore Network and Fluid Flow in Gas Shales. *SPE124253*.
- Wei, M., Duan, Y., Fang, Q., Wang, R., Yu, B., & Yu, C. (2013). Mechanism Model for Shale Gas Transport Considering Diffusion, Adsorption/Desorption and Darcy Flow. *Springer*.
- Xiong, X., Devegowda, D., Michel, G., & Civan, F. (2012). A Fully Coupled Free and Adsorptive Phase Transport Model for Shale Gas Reservoirs Including Non Darcy Flow Effect.

APPENDIX

Table 0.1 Sensitivity study table of pressure parameter on first level of modelling, K

Pore Pressure, Psia	Pore pressure, Pa	Pore hydraulic radius, nm	Intrinsic permeability, nD	Mean free path, nm	Knudsen number	Rarefaction coefficient	f(Kn)	Apparent Permeability (K), nD
500	3447378.645	1	0.125	2.184895733	2.184895733	68.85408374	566.99848352217	70.87481044
1000	6894757.29	1	0.125	1.092447867	1.092447867	66.08470066	226.04994685526	28.25624336
1500	10342135.94	1	0.125	0.728298578	0.728298578	64.11576419	128.09010840782	16.01126355
2000	13789514.58	1	0.125	0.546223933	0.546223933	62.543811	84.84999074171	10.60624884
2500	17236893.23	1	0.125	0.436979147	0.436979147	61.21842136	61.50722115087	7.688402644
3000	20684271.87	1	0.125	0.364149289	0.364149289	60.06436266	47.29484321447	5.911855402
3500	24131650.52	1	0.125	0.312127962	0.312127962	59.03778226	37.91278627903	4.739098285
4000	27579029.16	1	0.125	0.273111967	0.273111967	58.11054202	31.34729266865	3.918411584
4500	31026407.81	1	0.125	0.242766193	0.242766193	57.26334792	26.54532657336	3.318165822
5000	34473786.45	1	0.125	0.218489573	0.218489573	56.48230868	22.90944440339	2.86368055

Table 0.2 Sensitivity analysis of pressure parameter at Second level of modelling, Ka

Pore Pressure, psia	Pore Pressure, Pa	Hydraulic pore radius, nm	Effective radius, nm	Mean free path, nm	Kn'	Rarefaction coefficient	f(Kn')	Effective porosity	Adsorption modified intrinsic permeability, nD	Apparent Permeability (Ka), nD
500	3447378.645	1	0.91739130	2.18489573	2.38163990	69.15159247	632.47824890	0.84160681	0.08853775	55.99820224497
1000	6894757.29	1	0.86428571	1.09244787	1.26398927	66.72685253	275.92844874	0.74698980	0.06974922	19.24579391007
1500	10342135.94	1	0.82727273	0.72829858	0.88036092	65.07122427	167.44150471	0.68438017	0.05854703	9.80320218526
2000	13789514.58	1	0.80000000	0.54622393	0.68277992	63.77617046	116.84091603	0.64000000	0.05120000	5.98225490063
2500	17236893.23	1	0.77906977	0.43697915	0.56089861	62.69502824	88.14896588	0.60694970	0.04604849	4.05912700981
3000	20684271.87	1	0.76250000	0.36414929	0.47757284	61.75739902	69.91761325	0.58140625	0.04225415	2.95430955842
3500	24131650.52	1	0.74905660	0.31212796	0.41669476	60.92378615	57.43118514	0.56108580	0.03935216	2.26004111561
4000	27579029.16	1	0.73793103	0.27311197	0.37010500	60.16967975	48.41172737	0.54454221	0.03706578	1.79441831668
4500	31026407.81	1	0.72857143	0.24276619	0.33320850	59.47874425	41.63179821	0.53081633	0.03522075	1.46630301392
5000	34473786.45	1	0.72058824	0.21848957	0.30321002	58.83949438	36.37495529	0.51924740	0.03370223	1.22591723415

Table 0.3 Viscosity calculation for different pore pressure

Pore Pressure, Psia	Gas gravity	Gas compressibility factor	Density, g/cc	K	X	y	Viscosity, cp
500	0.553733559	0.969071003	0.019625549	132.724402	5.175557886	1.295955926	0.013700387
1000	0.553733559	0.939144367	0.040501867	132.724402	5.175557886	1.295955926	0.014394454
1500	0.553733559	0.911010735	0.062628956	132.724402	5.175557886	1.295955926	0.015309257
2000	0.553733559	0.884513657	0.086006814	132.724402	5.175557886	1.295955926	0.016461866
2500	0.553733559	0.859514369	0.110635442	132.724402	5.175557886	1.295955926	0.017888353
3000	0.553733559	0.835889365	0.136514839	132.724402	5.175557886	1.295955926	0.019640653
3500	0.553733559	0.813528354	0.163645006	132.724402	5.175557886	1.295955926	0.021788434
4000	0.553733559	0.792332538	0.192025943	132.724402	5.175557886	1.295955926	0.024423358
4500	0.553733559	0.772213156	0.22165765	132.724402	5.175557886	1.295955926	0.027665553
5000	0.553733559	0.753090238	0.252540126	132.724402	5.175557886	1.295955926	0.031672800

Table 0.4 Sensitivity analysis on pressure parameter on third level of modelling, Kad

Pore Pressure, Psia	Pore Pressure, Psig	Temp, R	Molecular weight, lb/lbmol	Surface diffusivity, cm ² /s	Viscosity, cp	Adsorbed phase concentration, mol/cc	Langmuir pressure, Psia	Effective porosity	Apparent Permeability (Ka), nD	Apparent Permeability (Kad), nD
500	485.3	630	16.04	0.008184416	0.013700387	0.02504	1800	0.841606805	55.99820224497	55.99820224739
1000	985.3	630	16.04	0.003984461	0.014394454	0.02504	1800	0.746989796	19.24579391007	19.24579391141
1500	1485.3	630	16.04	0.002579411	0.015309257	0.02504	1800	0.684380165	9.80320218526	9.80320218609
2000	1985.3	630	16.04	0.001872137	0.016461866	0.02504	1800	0.640000000	5.98225490063	5.98225490118
2500	2485.3	630	16.04	0.001443243	0.017888353	0.02504	1800	0.606949703	4.05912700981	4.05912701021
3000	2985.3	630	16.04	0.001152950	0.019640653	0.02504	1800	0.581406250	2.95430955842	2.95430955872
3500	3485.3	630	16.04	0.000941370	0.021788434	0.02504	1800	0.561085796	2.26004111561	2.26004111584
4000	3985.3	630	16.04	0.000778570	0.024423358	0.02504	1800	0.544542212	1.79441831668	1.79441831687
4500	4485.3	630	16.04	0.000647932	0.027665553	0.02504	1800	0.530816327	1.46630301392	1.46630301407
5000	4985.3	630	16.04	0.000539490	0.031672800	0.02504	1800	0.519247405	1.22591723415	1.22591723428

Table 0.5 Sensitivity analysis on pore size parameter on first level of modelling, K

Pore hydraulic radius, nm	Pore Pressure, Psia	Pore pressure, Pa	Intrinsic permeability, nD	Mean free path, nm	Knudsen number	Rarefaction coefficient	f(Kn)	Apparent Permeability (K), nD
1	500	3447378.645	0.125	2.184895733	2.184895733	68.85408374	566.99848352217	70.87481044
2	500	3447378.645	0.500	2.184895733	1.092447867	66.08470066	226.04994685526	113.0249734
3	500	3447378.645	1.125	2.184895733	0.728298578	64.11576419	128.09010840782	144.101372
4	500	3447378.645	2.000	2.184895733	0.546223933	62.54381100	84.84999074171	169.6999815
5	500	3447378.645	3.125	2.184895733	0.436979147	61.21842136	61.50722115087	192.2100661
6	500	3447378.645	4.500	2.184895733	0.364149289	60.06436266	47.29484321447	212.8267945
7	500	3447378.645	6.125	2.184895733	0.312127962	59.03778226	37.91278627903	232.215816
8	500	3447378.645	8.000	2.184895733	0.273111967	58.11054202	31.34729266865	250.7783413
9	500	3447378.645	10.125	2.184895733	0.242766193	57.26334792	26.54532657336	268.7714316
10	500	3447378.645	12.500	2.184895733	0.218489573	56.48230868	22.90944440339	286.368055

Table 0.6 Sensitivity analysis on pore size parameter on second level of modelling, Ka

Hydraulic pore radius, nm	Pore Pressure, Psia	Pore Pressure, Pa	Effective radius, nm	Mean free path, nm	Kn'	Rarefaction coefficient	f(Kn')	Effective porosity	Adsorption modified intrinsic permeability, nD	Apparent Permeability, (Ka), nD
1	500	3447378.645	0.91739130	2.18489573	2.38163990	69.15159247	632.47824890	0.84160681	0.08853775	55.99820224497
2	500	3447378.645	1.91739130	2.18489573	1.13951478	66.27387532	239.53971501	0.91909735	0.42236997	101.17438286678
3	500	3447378.645	2.91739130	2.18489573	0.74892104	64.26039623	133.27262560	0.94568578	1.00611179	134.08716049426
4	500	3447378.645	3.91739130	2.18489573	0.55774253	62.66295246	87.43642484	0.95912216	1.83983065	160.86821458595
5	500	3447378.645	4.91739130	2.18489573	0.44432009	61.32065803	63.00357319	0.96722949	2.92354027	184.19348321221
6	500	3447378.645	5.91739130	2.18489573	0.36923293	60.15439703	48.24765870	0.97265333	4.25724524	205.40211553110
7	500	3447378.645	6.91739130	2.18489573	0.31585545	59.11850828	38.56188834	0.97653678	5.84094756	225.23796780632
8	500	3447378.645	7.91739130	2.18489573	0.27596157	58.18388528	31.81226801	0.97945445	7.67464822	244.14796610532
9	500	3447378.645	8.91739130	2.18489573	0.24501512	57.33066366	26.89159706	0.98172676	9.75834777	262.41755621558
10	500	3447378.645	9.91739130	2.18489573	0.22030952	56.54459203	23.17541687	0.98354650	12.09204654	280.23821942772

Table 0.7 Viscosity calculation for different pore sizes

Hydraulic Pore radius, nm	Gas gravity	Gas compressibility factor	Density, g/cc	K	X	y	Viscosity, cp
1	0.553733559	0.969071003	0.019625549	132.724402	5.175557886	1.295955926	0.013700387
2	0.553733559	0.969071003	0.019625549	132.724402	5.175557886	1.295955926	0.013700387
3	0.553733559	0.969071003	0.019625549	132.724402	5.175557886	1.295955926	0.013700387
4	0.553733559	0.969071003	0.019625549	132.724402	5.175557886	1.295955926	0.013700387
5	0.553733559	0.969071003	0.019625549	132.724402	5.175557886	1.295955926	0.013700387
6	0.553733559	0.969071003	0.019625549	132.724402	5.175557886	1.295955926	0.013700387
7	0.553733559	0.969071003	0.019625549	132.724402	5.175557886	1.295955926	0.013700387
8	0.553733559	0.969071003	0.019625549	132.724402	5.175557886	1.295955926	0.013700387
9	0.553733559	0.969071003	0.019625549	132.724402	5.175557886	1.295955926	0.013700387
10	0.553733559	0.969071003	0.019625549	132.724402	5.175557886	1.295955926	0.013700387

Table 0.8 Sensitivity analysis on pore size parameter on third level of modelling, Kad

Hydraulic Pore radius nm	Pore Pressure, Psia	Pore Pressure, Psig	Temp, R	Molecular weight, lb/lbmol	Surface diffusivity, cm ² /s	Viscosity, cp	Adsorbed phase concentration, mol/cc	Langmuir pressure, Psia	Effective porosity	Apparent Permeability Ka,nD	Apparent Permeability (Kad), nD
1	500	485.3	630	16.04	0.008184416	0.013700387	0.02504	1800	0.841606805	55.99820224497	55.99820224739
2	500	485.3	630	16.04	0.008184416	0.013700387	0.02504	1800	0.919097353	101.17438286678	101.17438286802
3	500	485.3	630	16.04	0.008184416	0.013700387	0.02504	1800	0.945685780	134.08716049426	134.08716049509
4	500	485.3	630	16.04	0.008184416	0.013700387	0.02504	1800	0.959122164	160.86821458595	160.86821458658
5	500	485.3	630	16.04	0.008184416	0.013700387	0.02504	1800	0.967229490	184.19348321221	184.19348321271
6	500	485.3	630	16.04	0.008184416	0.013700387	0.02504	1800	0.972653329	205.40211553110	205.40211553152
7	500	485.3	630	16.04	0.008184416	0.013700387	0.02504	1800	0.976536785	225.23796780632	225.23796780668
8	500	485.3	630	16.04	0.008184416	0.013700387	0.02504	1800	0.979454454	244.14796610532	244.14796610564
9	500	485.3	630	16.04	0.008184416	0.013700387	0.02504	1800	0.981726761	262.41755621558	262.41755621586
10	500	485.3	630	16.04	0.008184416	0.013700387	0.02504	1800	0.983546503	280.23821942772	280.23821942798

Table 0.9 Sensitivity analysis on temperature parameter on first level of modelling, K

Temperature, K	Pore Pressure, Psia	Pore pressure, Pa	Pore hydraulic radius, nm	Intrinsic permeability, nD (K_{∞})	Mean free path, nm	Knudsen number	Rarefaction coefficient	f(Kn)	Apparent Permeability (K), nD
310	500	3447378.645	1	0.125	1.935193364	1.935193364	68.41873769	485.21886836833	60.65235855
315	500	3447378.645	1	0.125	1.96640616	1.96640616	68.47726684	495.35010367594	61.91876296
320	500	3447378.645	1	0.125	1.997618956	1.997618956	68.53453512	505.50886359374	63.18860795
325	500	3447378.645	1	0.125	2.028831753	2.028831753	68.59058848	515.69438113920	64.46179764
330	500	3447378.645	1	0.125	2.060044549	2.060044549	68.64547052	525.90591894246	65.73823987
335	500	3447378.645	1	0.125	2.091257345	2.091257345	68.69922264	536.14276780786	67.01784598
340	500	3447378.645	1	0.125	2.122470141	2.122470141	68.75188422	546.40424535907	68.30053067
345	500	3447378.645	1	0.125	2.153682937	2.153682937	68.8034927	556.68969476229	69.58621185
350	500	3447378.645	1	0.125	2.184895733	2.184895733	68.85408374	566.99848352217	70.87481044
355	500	3447378.645	1	0.125	2.21610853	2.21610853	68.90369131	577.33000234574	72.16625029

Table 0.10 Sensitivity analysis on temperature parameter on second level of modelling, Ka

Temp, K	Pore Pressure, psia	Pore Pressure, Pa	Effective radius, nm	Mean free path, nm	Kn'	Rarefaction coefficient	f(Kn')	Effective porosity	Adsorption modified intrinsic permeability, nD	Apparent Permeability (Ka), nD
310	500	3447378.645	0.91739130	1.93519336	2.10945248	68.73005122	542.12162581	0.84160681	0.08853775	47.99822997314
315	500	3447378.645	0.91739130	1.96640616	2.14347591	68.78672965	553.32360805	0.84160681	0.08853775	48.99002829647
320	500	3447378.645	0.91739130	1.99761896	2.17749934	68.84218550	564.55356529	0.84160681	0.08853775	49.98430346379
325	500	3447378.645	0.91739130	2.02883175	2.21152276	68.89646335	575.81070002	0.84160681	0.08853775	50.98098486463
330	500	3447378.645	0.91739130	2.06004455	2.24554619	68.94960554	587.09424631	0.84160681	0.08853775	51.98000468603
335	500	3447378.645	0.91739130	2.09125734	2.27956962	69.00165225	598.40346826	0.84160681	0.08853775	52.98129777302
340	500	3447378.645	0.91739130	2.12247014	2.31359304	69.05264170	609.73765852	0.84160681	0.08853775	53.98480149735
345	500	3447378.645	0.91739130	2.15368294	2.34761647	69.10261024	621.09613686	0.84160681	0.08853775	54.99045563400
350	500	3447378.645	0.91739130	2.18489573	2.38163990	69.15159247	632.47824890	0.84160681	0.08853775	55.99820224497
355	500	3447378.645	0.91739130	2.21610853	2.41566333	69.19962134	643.88336484	0.84160681	0.08853775	57.00798556969

Table 0.11 Viscosity calculation for different temperatures

Temperature, K	Gas gravity	Gas compressibility factor	Density, g/cc	K	X	y	Viscosity, cp
310	0.553733559	0.951682537	0.022562731	118.0368382	5.377585535	1.251024977	0.012369751
315	0.553733559	0.954420216	0.0221409	119.9012822	5.34952614	1.257265387	0.012535003
320	0.553733559	0.956970112	0.021736875	121.7575245	5.3223436	1.263310783	0.012700754
325	0.553733559	0.959347021	0.021349434	123.605591	5.295997446	1.269170168	0.012866896
330	0.553733559	0.961564451	0.02097747	125.4455109	5.270449661	1.274851995	0.013033331
335	0.553733559	0.963634751	0.020619978	127.2773161	5.245664496	1.280364216	0.013199970
340	0.553733559	0.965569205	0.02027604	129.1010413	5.221608306	1.285714313	0.013366738
345	0.553733559	0.967378139	0.019944819	130.9167235	5.198249397	1.290909334	0.013533564
350	0.553733559	0.969071003	0.019625549	132.724402	5.175557886	1.295955926	0.013700387
355	0.553733559	0.970656454	0.019317528	134.5241179	5.153505572	1.300860361	0.013867151

Table 0.12 Sensitivity analysis of temperature parameter on third level of modelling, Kad

Temp, K	Temp, R	Pore Pressure, Psia	Pore Pressure, Psig	Molecular weight, lb/lbmol	Surface diffusivity, cm ² /s	Viscosity, cp	Adsorbed phase concentration, mol/cc	Langmuir pressure, Psia	Effective porosity	Apparent Permeability (Ka), nD	Apparent Permeability (Kad), nD
310	558	500	485.3	16.04	0.006544927	0.012369751	0.02504	1800	0.841606805	47.99822997314	47.99822997489
315	567	500	485.3	16.04	0.006743922	0.012535003	0.02504	1800	0.841606805	48.99002829647	48.99002829830
320	576	500	485.3	16.04	0.006944598	0.012700754	0.02504	1800	0.841606805	49.98430346379	49.98430346570
325	585	500	485.3	16.04	0.007146963	0.012866896	0.02504	1800	0.841606805	50.98098486463	50.98098486662
330	594	500	485.3	16.04	0.007351026	0.013033331	0.02504	1800	0.841606805	51.98000468603	51.98000468810
335	603	500	485.3	16.04	0.007556796	0.013199970	0.02504	1800	0.841606805	52.98129777302	52.98129777518
340	612	500	485.3	16.04	0.007764279	0.013366738	0.02504	1800	0.841606805	53.98480149735	53.98480149959
345	621	500	485.3	16.04	0.007973484	0.013533564	0.02504	1800	0.841606805	54.99045563400	54.99045563634
350	630	500	485.3	16.04	0.008184416	0.013700387	0.02504	1800	0.841606805	55.99820224497	55.99820224739
355	639	500	485.3	16.04	0.008397081	0.013867151	0.02504	1800	0.841606805	57.00798556969	57.00798557221

